

Real-Time Volumetric Phase Monitoring: Advancing Chemical Analysis by Countercurrent Separation

Guido F. Pauli,^{*,†,‡} Samuel M. Pro,[§] Lucas R. Chadwick,[§] Thomas Burdick,[§] Luke Pro,[§] Warren Friedl,[§] Nick Novak,[§] John Maltby,[§] Feng Qiu,[†] and J. Brent Friesen^{†,‡,⊥}

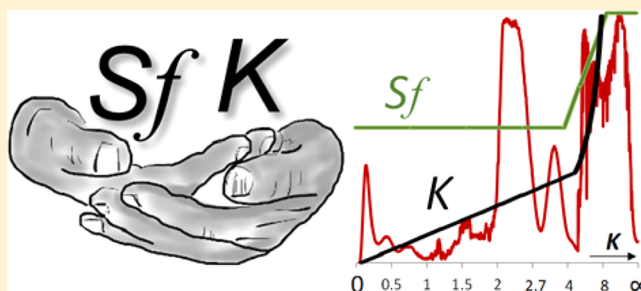
[†]Department of Medicinal Chemistry and Pharmacognosy and [‡]Institute for Tuberculosis Research, College of Pharmacy, University of Illinois at Chicago, Chicago, Illinois 60612, United States

[§]Cherry Instruments, 1134 West Granville Avenue, Suite 1109, Chicago, Illinois 60660, United States

[⊥]Physical Sciences Department, Dominican University, River Forest, Illinois 60305, United States

S Supporting Information

ABSTRACT: Countercurrent separation (CCS) utilizes the differential partitioning behavior of analytes between two immiscible liquid phases. We introduce the first platform ("CherryOne") capable of real-time monitoring, metering, and control of the dynamic liquid–liquid CCS process. Automated phase monitoring and volumetrics are made possible with an array of sensors, including the new permittivity-based phase metering apparatus (PMA). Volumetric data for each liquid phase are converted into a dynamic real-time display of stationary phase retention (S_f) and eluent partition coefficients (K), which represent critical parameters of CCS reproducibility. When coupled with the elution–extrusion operational mode (EECCC), automated S_f and K determination empowers untargeted and targeted applications ranging from metabolomic analysis to preparative purifications.



Countercurrent chromatography (CCC) and centrifugal partition chromatography (CPC), collectively called countercurrent separation (CCS), are liquid-only chromatographic methods with a long history of development and use.^{1,2} In CCS, the partition coefficient (K) is similar to the gas chromatography retention index (RI) in that it is a commonly reported chromatographic metric that normalizes results and minimizes the impact of experimental variables. However, for K there exists a true value, which is a fundamental thermodynamic property of analytes and solvents. While CCS operates at much lower pressures, both CCS and the omnipresent (U)HPLC are liquid chromatography (LC) techniques that employ a liquid mobile phase. This common feature may explain the general tendency to apply or adapt (HP)LC tools for CCS operation. While certain peripherals are common to both forms of LC (pump, detector, and autosampler), as are some operational parameters such as flow rate and temperature, the liquid stationary phase (column) in CCS entails additional operational parameters such as rotation speed, rotation direction, and flow direction. The additional complexity introduced by these factors largely explains why CCS has not been more widely adopted.

Common to all CCS methods is column equilibration, which involves pumping the mobile phase into the CCS column filled with stationary phase until a dynamic equilibrium is reached between the stationary and mobile phases and quantified as the stationary phase retention (S_f).³ However, loss of stationary phase during the chromatographic process is a common

phenomenon in CCS practice and is influenced by sample matrix and loading conditions.³ Typically, stationary phase loss occurs when the sample enters the column, but may occur at any point during the separation process. This is especially true when the sample causes emulsions and/or the sample loading increases. Because an accurate measure of stationary and mobile phase volumes is a prerequisite for the calculation of K values, it is necessary to carefully monitor stationary phase loss during the chromatographic process. To date, few hardware peripherals and acquisition/processing software are designed to support CCS instruments. Importantly, because key CCS parameters (S_f and K) are mostly ignored, achieving a reasonable level of accuracy and precision requires manual intervention by a skilled operator.

The design of modern automated CCS systems must confront a number of challenges: (i) both phases (mobile and stationary) in CCS are entirely determined by solvent composition, (ii) volumetrics drive CCS data quality, (iii) stationary phase retention (S_f) is a critical and dynamic variable in CCS, (iv) accuracy of partition coefficient (K) measurements hinges on the accuracy of S_f measurements, and (v) there are several relatively unfamiliar operational parameters in CCS. While these challenges can be partially addressed through

Received: April 28, 2015

Accepted: June 3, 2015

Published: July 8, 2015

education and familiarity with CCS operation, automation of the Sf measurement and real-time, precise calculation of K remains a true technological challenge.

(i) CCS can employ a virtually limitless range of *biphasic* solvent systems, which can make their efficient selection for any given separation a daunting task for the analyst unfamiliar with CCS. Typically, solvent systems are comprised of two- to six-component mixtures. While their principal constitution and nomenclature are established in the literature (see refs 1 and 2 and references therein; summary for the present study in section SI1, Supporting Information), selection remains largely an empirical task unless target K values are known or predictable. Thus, methods and tools to streamline the selection and use of solvents must be incorporated into modern CCS systems.

(ii) Most often, CCS chromatograms are represented with elution time on the x -axis. However, in CCS, retention *volumes* are more important than retention *times*. In addition, due to the dynamic nature of Sf, as well as inter-instrument differences, retention volumes alone are *not enough* for documentation or reporting and can be misleading when comparing results or, most importantly, when calculating eluent K values. Therefore, CCS volumetrics should include extracolumn volumes and/or stationary phase loss in the correct calculation of K values.^{3,4}

(iii) In CCS, it is critical to monitor the (dynamic!) displacement of the stationary phase. Determination of Sf is a fundamental task of the countercurrent chromatographer. However, the occurrence of stationary phase loss during the run (sometimes referred to as column “bleeding”) makes Sf a dynamic variable that is rather challenging and/or laborious to measure manually. A unique requirement for the automation of CCS is the need to know what chromatographic phase is exiting the column at any given moment: mobile phase, stationary phase, or some combination of the two. This information is indispensable for accurate determination of Sf values, which, in turn, are required to either accurately calculate eluent K values or, conversely, to predict when an analyte will elute from the column. The calculation enables K -based chromatograms that, unlike widespread time or elution volume plots, are reproducible and independent of instruments and runs. The only variables impacting the location of the peak center are the solvents and the sample. To date, the Sf value is typically determined by a manual volumetric measurement carried out at a single time point. However, in practice, stationary phase may be lost at any point in the run after sample injection, thereby steadily decreasing the real-time Sf relative to the initial value.

Surprisingly, while the dynamic nature of Sf in CCS practice is well-known, it is often ignored as the technology required to measure stationary phase loss has been unavailable and a manual approach is unfeasible. For a CCS column, the Sf value is the volume of the stationary phase (V_S) divided by the total column volume (V_C). However, the volume of the stationary phase is often measured indirectly as the difference of V_C and the mobile phase volume (V_M) as shown in eq 1.⁵

$$Sf = V_S/V_C = (V_C - V_M)/V_C \quad (1)$$

As will be shown in the results, section I2, the three established manual methods for Sf measurement do not always agree with one another. The discrepancy is due to loss of stationary phase during the chromatographic separation. It is precisely this phenomenon that engenders a difference between actual K values and CCS-observed K values. In cases where the actual Sf

value at the moment of analyte elution is less than the observed Sf value ($Sf_{\text{actual}} < Sf_{\text{observed}}$), the observed K values will be greater than the actual K values for analytes with $K < 1$. Conversely, for analytes with $K > 1$ and $Sf_{\text{actual}} < Sf_{\text{observed}}$, the observed K value will be less than the actual K values. For all established (nonautomated) methods to measure Sf, the injection before equilibration (IBE) operational mode⁶ produces the most accurate Sf value under high sample loading conditions. It is important to note that, in work with a small-volume column, extra column volume of the tubing both before and after the column as well as the sample injection volume must be taken into account when making careful Sf calculations.⁴

(iv) Liquid–liquid partition coefficients (K values) are thermodynamic properties of the analyte and the solvent system and are essential for normalization of CCS results. In CCS, an accurate measurement of Sf is necessary for an accurate determination of K values from known V_R , or for prediction of V_R from known K values. The accuracy of CCS eluent K values depends primarily on the accuracy of Sf measurements. In fact, CCS becomes highly predictable once K and Sf are known.^{1,2,7,8} Thus, while real-time knowledge of K can enable predictable and targeted separations,^{8–10} mainstream CCS technology does not support this capability by providing K as output (K -based chromatograms) in real time. In fact, this precludes the broader implementation of a standardized form of CCS chromatograms, such as normal and shifted reciprocal symmetry plots (ReS and ReSS, respectively),¹¹ in which the x -axis is normalized to K -values. Without real-time knowledge of Sf, K values can only be determined after the fact and with lower accuracy, dictated by the practical inability to accurately determine phase volumes over time. However, with accurate volumetrics, the elution volume (known as retention volume) V_R , of an analyte is expressed by the equation $V_R = V_M + KV_S$, or rearranged⁵

$$K = (V_R - V_M)/V_S \quad (2)$$

where, notably, K is *also* the ratio of solute concentration in the stationary phase over the concentration in the mobile phase at equilibrium at a given temperature.

(v) Numerous CCS operational modes have been developed and are widely used including the following: EECCC,¹² pH-zone refining,¹³ BECCC,¹⁴ dual mode,¹⁵ solvent gradient elution,¹⁶ and flow rate gradient elution.¹⁷ Their automation requires real-time knowledge of core CCS parameters, especially Sf. In the widely used EECCC method, the solute retention volume, V_{EECCC} , becomes $V_{\text{EECCC}} = V_{\text{CM}} + V_C - V_{\text{CM}}/K$, for solutes with $K > V_{\text{CM}}/V_S$, i.e., during EECCC stage III (extrusion), or solving for K ,¹²

$$K = V_{\text{CM}}/(V_{\text{CM}} + V_C + V_{\text{EECCC}}) \quad (3)$$

where V_{CM} represents the volume of mobile phase passed through the column before the stationary phase is pumped into the column.

Together, these five points outline what ultimately generates the challenge of parametrization and automation in CCS. Due to both the liquid-only and dynamic nature of the CCS experiment, full knowledge and/or control over the entire set of parameters that impact its volumetrics become the prerequisite for the level of automation required for a new generation of CCS instrumentation, such as the CherryOne instrument developed herein (see section SI3, Supporting Information). Thus, CCS automation involves real-time monitoring and

programmable control that provides ease of operation (plug and play strategies) and feedback of CCS critical parameters. Ease of operation is promoted by standardized methods controlled by software components. The present study introduces real-time CCS volumetrics and provides the blueprint for a fully integrated CCS platform that offers the unique potential of *K* targeting. This elevates the reproducibility of CCS and enables a level of automation that has the potential to move CCS from a “last resort” technique to a mainstream chromatographic method.

EXPERIMENTAL SECTION

CCS Instrumentation, Solvent Delivery, and Operational Parameters. HSCCC was performed on a TBE-20A high-speed countercurrent chromatograph (Tauto Biotech, Shanghai, China), equipped with a 17.9 mL coil of 0.8 mm i.d. PTFE tubing; experiments with an 80 mL column used a Sanki centrifugal partition chromatograph (CPC; Sanki Engineering Ltd., Tokyo, Japan). The HSCCC operating and solvent delivery system was equipped with a six-port valve, 0.5 mL sample loop, a custom designed multipump array, UV detector, pressure sensor, phase metering apparatus (PMA, see later text), temperature sensor, and a specialized software control interface. Fraction collection was accomplished with a Foxy Jr. fraction collector (Teledyne Isco, Lincoln, NE, USA). Sensor development was performed with a PerkinElmer 200 series pump (lag volume, 2–6 mL, depending on solvent) with quaternary gradient mixer module (see also section SI8, Supporting Information). Section SI11 of the Supporting Information provides further operational parameters.

Plant Extracts. A xanthohumol-enriched hops extract (*Humulus lupulus* L.) provided by Hopsteiner (S. S. Steiner, Inc., New York, NY, USA)⁹ was used to study the impact of sample loading on stationary phase loss, using the previously described 17.9 mL HSCCC instrument. The catechin-enriched green tea extract was obtained from Naturex (South Hackensack, NJ, USA).

Development of Phase Metering Apparatus. First, a solvent interface apparatus (SIA) was devised to deliver precise and repeatable amounts of solvents to the candidate PMA sensors. The SIA consisted of a three-syringe pump (modified Zymark ZS10 Master Laboratory Station), controlled by custom software written in the Python programming language, and a data acquisition unit composed of a National Instruments PCI-6251 card.

The following devices and sensors were adapted for the purpose of flow-through liquid sensing and evaluated for their ability to discriminate the solvent phases. The optical (video) sensor consisted of a Canon HF100 3.3 MP HD CMOS device. The mass flow sensor was adapted from a SensirionASL 1600 thermometric CMOS sensor (Sensirion AG, Staefa, Switzerland). The UV sensor was adapted from a PerkinElmer series 200 HPLC detector. The pressure sensor consisted of an Omega PX409 high-accuracy piezoresistor (OMEGA Engineering, Inc., Stamford, CT, USA). The permittivity-based sensor consisted of conductive material wound orthogonal to the flow path and was built specifically for this CCS application.

PMA Data Collection. The acquisition of baseline PMA signal values of biphasic solvent systems involved pumping each discrete phase directly through the PMA device. First, the upper phase was pumped at 2 mL/min for 3 min and then the flow rate was reduced to 1 mL/min for 1 min before being switched to the lower phase at 2 mL/min for 3 min. Finally, the

flow rate was reduced to 1 mL/min for 1 min. The experiment was then repeated with the opposite order, first the lower and then the upper phase. PMA signal values were recorded, displayed (Supporting Information Figure SI4a,b), and saved as *.csv files for later inspection.

RESULTS AND DISCUSSION

Development (D1–D6) of Phase Sensor Technology.

The use of a phase sensing device for real-time monitoring of eluting immiscible solvent system phases in CCS has not been reported. Therefore, in order to provide real-time measurement of the eluent, five prototype sensors were investigated: optical (video), thermal mass flow, UV absorbance, pressure (viscosity), and permittivity. It was demonstrated that each of these sensing technologies could be used to monitor key CCS volumetric data in real time. The most promising sensors were a high-accuracy pressure transducer and a permittivity sensor.

D1: Solvent Interface Apparatus. Subsequent studies involved the use of a SIA that was capable of precisely delivering alternating plugs of solvent phases in volumes as low as 1 μ L. A multistage SIA program was used to evaluate and rank potential sensors: As illustrated in Figure 1, “Stage I”

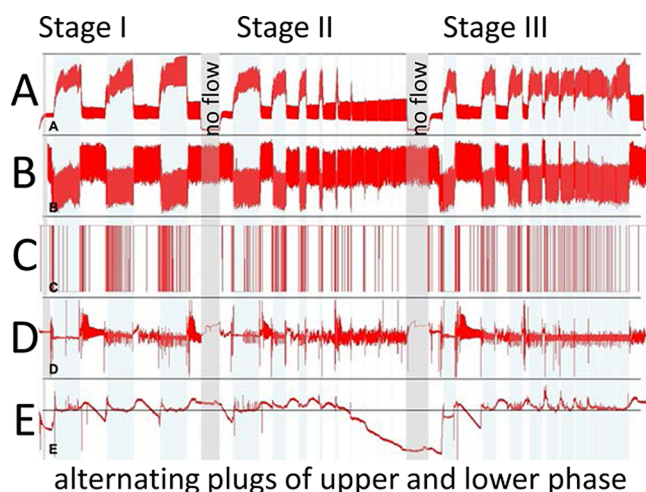


Figure 1. Results for each sensor tested with the solvent interface apparatus (SIA) using the HEMWat 0 (hexane/ethyl acetate/methanol/water (1:1:1:1)) solvent system: A, pressure; B, permittivity; C, visual; D, mass flow; E, UV. The solvent interface apparatus sensor testing protocol can be found in section SI5, Supporting Information.

served as a calibration and baseline routine, while “Stage II” delivered increasingly small plugs of upper phase in a steady stream of lower phase, and “Stage III” delivered increasingly small plugs of lower phase in a steady stream of upper phase (for protocols and results, see sections SI5 and SI6, Supporting Information).

D2: Optical Sensor. A flow cell was designed for optimal visualization of immiscible liquid phases passing through it. A customized light box in conjunction with a borosilicate glass capillary (1.5 mm o.d., 1.12 mm i.d.) was used to investigate lighting and background conditions that allowed visual discrimination of the phases. High-intensity fluorescent lighting, alongside a simple high-contrast background with both vertical and horizontal elements, provided the best results. This optimized apparatus was coupled with a high-quality CMOS video sensor and macrolens. Subsequently, this sensor provided

a visual tool to aid in the understanding of the characteristics of biphasic flow through a capillary flow cell (see Figure SI4a, Supporting Information). Figure 1C shows a representation of visual results from the stages I, II, and III testing for the HEMWat 0 (*n*-hexane/EtOAc/MeOH/H₂O (1:1:1:1)) solvent system (see section SI1 Supporting Information).

The optical sensor showed a clear ability to distinguish between phases, but the associated data and processing costs of this apparatus were significantly higher than for most other candidates. However, when coupled with CCS, the video signal provides a unique real-time perspective for the operator. Solvent plugs of at least 8 μ L are easy to identify by the human observer. This sensor was important in identifying the magnitude of the pump "lag volume" and understanding of column extrusion studies described in implementation 1. The sensitivity of an optical sensor may be enhanced by incorporating a dye into one of the phases.¹⁸

D3: Mass Flow Sensor. The mass flow sensor was constructed with a commercially available thermometric CMOS sensor. While it showed good results for HEMWat 0 and BuAaWat, it was incapable of distinguishing between the immiscible phases the HepAc and ATPS solvent systems (see section SI6, Supporting Information). Figure 1D shows that the mass flow sensor signal for the HEMWat 0 solvent system was challenging to correlate with eluent composition. Not surprisingly, however, the signal was readily correlated with total solvent flow.

D4: UV Detector. Most solvents absorb at 190 nm with the absorptivity values varying widely from one solvent to another. However, the data for the sensor evaluation of the HEMWat 0 solvent system Figure 1E suggest the response time is rather poor and does not appear to correlate with volumetric measurements. The UV detector as tested, therefore, was not an effective phase sensor. However, in practice, interpretation of the UV signal is enhanced by the PMA, as shown in Figure SI7c,d of section SI7, Supporting Information. The performance of this detector, as a phase sensor candidate, could likely be improved by modifying the flow cell to better accommodate biphasic systems and removing the integrated signal processing/smoothing which is optimized for analyte peaks. These modifications however would likely decrease its performance as an analyte detector.

D5: Pressure/Viscosity Sensor. The pressure sensor, based on a commercially available high-accuracy piezoresistor, was coupled with a fixed postsensor flow restriction element (100 psi back-pressure regulator). This restriction created variable back-pressure proportional to the viscosity of the liquid flowing through it. Figure 1A and Supporting Information Figure SI4b show that, under these conditions, the pressure sensor was able to readily distinguish between the upper and lower phases in five different solvent systems studied. However, the flow restriction requirement of this sensor causes complications with higher flow rates typically used to fill and clean CCS columns, and introduced a potential clogging point.

D6: Permittivity Sensor. Designed to continuously measure dielectric behavior of liquid passing through it, the performance of the permittivity sensor was influenced by its construction materials and the electronics used to acquire the signal. This sensor produces an electrical field through its flow cell. Changes in the dielectric properties of the liquid within the cell alter its resonating frequency. Measurements of this frequency (Hz), along with temperature, are continuously outputted from the sensor and correlate logarithmically to the relative static

permittivity of the flow cell contents (Figure SI7e, Supporting Information). The relative static permittivity of a solvent is a dimensionless number (ratio of permittivities) and an effective measure of its polarity as represented by its dielectric constant.^{19–22} Investigating HEMWat 0 with an early prototype of the sensor (Figure 1B) indicated it could accommodate high flow rates, did not interfere with the liquid flow path, and was capable of distinguishing between immiscible solvent phases. This sensor was found to be effective for a wide range of solvent systems, whereas its capabilities are diminished by solvent systems containing ionic or ionizable components, such as BuAaWat and ATPS.

Implementation (I1–I4) of Phase Sensing into an Instrument for CCS Automation. Representative signals obtained with each of the five sensors for HEMWat 0 are shown in Figure 1. The outcome highlights the distinct capacity of both the pressure and permittivity sensors to detect increasingly small plugs of the immiscible phases. Both sensors detected plugs of 100 μ L and smaller (<10 μ L) for a variety of solvent systems. The sensors' limits of detection were lower than what can be achieved manually by a skilled operator and, therefore, deemed the best for obtaining the most reproducible real-time Sf information; better than has been previously achievable. Section SI6 of the Supporting Information summarizes the overall effectiveness of each sensor to distinguish between immiscible phases of each solvent system tested. HEMWat is the most widely used single CCS solvent system family¹ and fully amenable to volumetric monitoring by all sensors evaluated. For the realization of a new automated CCS instrument, the permittivity sensor was considered to be the best sensor overall based on the following: (i) its ability to distinguish between phases of a wide variety of biphasic systems, (ii) its facility to be placed directly online with the CCS effluent, (iii) the relatively low cost of its hardware, and (iv) the simplicity of signal analysis.

After evaluating potential technologies for discrimination of solvent phases, the implementation stage of the project consisted of two parallel steps: (1) studying the effect of sample loading on the dynamic CCS system and (2) the effect of stationary phase loss on the determination of *K* values. The results showed that phase sensing technology enabled both the optimization of sample loading and recognition of stationary phase loss during operation, and also enabled reproducible and automated calculation of analyte *K* values.

I1: Testing the Permittivity Sensor on a CCS Instrument. When switching between immiscible phases, all liquid pumps exhibit a lag volume until no more of the former phase is observed at the pump outlet, which confounds the precise switching between two immiscible phases for volumetric measurements. The lag volume is variable and depends on the miscibility of the solvents and whether the upper phase is displacing the lower phase or vice versa. To eliminate this variable and enable precise volumetrics, a purge valve was placed between the pump and the injection port to model a "perfect" binary pump, capable of switching between delivered phases with zero lag volume (see section SI8, Supporting Information). Next, a series of experiments were undertaken to compare the various methods of column filling (displacement of the one immiscible phase with another) required for efficient EECCC operation. Volumetric data were compiled from 13 experiments investigating the effect of column filling parameters on the replacement of phases (see section SI9, Supporting Information).

I2: Measurement of S_f and Its Impact on CCS-Based K -Value Determinations. The S_f calculations obtained by the three manual methods, described in section SI2 of the Supporting Information, converged at zero sample loading, but showed increasing divergence and variability at higher sample loading. For example, with 10 mg of hop extract loaded onto the 17.9 mL column, S_f measurements ranged from 0.28 to 0.41, depending on the method to measure V_M . According to the carryover-based $S_{f(CO)}$ value of 0.41, the predicted retention volume (V_R) of xanthohumol, with $K = 1.24$ in HEMWat 0,²³ would be 21.0 mL. On the other hand, mobile phase extrusion indicates the final $S_{f(MP)}$ value of 0.28, which equates to a predicted of xanthohumol V_R of 20.0 mL and already represents an unfavorable deviation (5%), even when considering a typical peak width. Importantly, the farther an analyte's K value is from unity, the larger this difference becomes. This essential lack of peak reproducibility illustrates the intrinsic limitation of being able to automate CCS in the absence of reliable real-time S_f measurement capabilities.

The three manual methods, described in section SI2 (Supporting Information), were systematically employed to assess variability in S_f measurements. Heavy loading produces a significant difference between these established methods. As shown in Figure 2, when the HEMWat solvent system was used

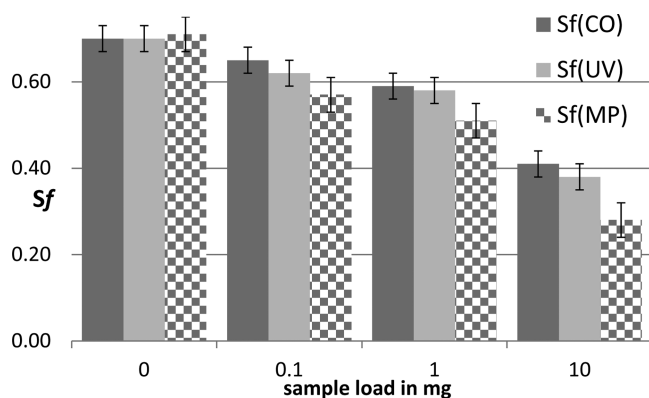


Figure 2. Results from loading studies where S_f (stationary phase volume ratio) was determined by three different methods: carryover (CO, dark gray) volume during equilibration; void volume detection (UV, light gray); extruding the mobile phase (MP, checkered). Experimental details can be found in section SI11, Supporting Information.

to its full loading capacity, the amount of stationary phase inside the column was reduced significantly below what is obtained by simply equilibrating a blank column (cf. experiments 1–3 vs higher-loading experiments in section SI11, Supporting Information; Figure 3). In addition to providing a more accurate S_f value (by either $S_{f(CO)}$ or $S_{f(UV)}$) than what is measured by simply equilibrating a blank column, the injection before equilibration operating mode has the added benefit of saving the time and solvents that would be expended in a separate equilibration step. However, the IBE operation cannot and does not account for continued reduction in S_f throughout the run. Therefore, the true value for S_f lies somewhere between $S_{f(CO)}$ and $S_{f(MP)}$. Considering the fundamental nature of analyte K and the impact of S_f on CCS-based determination of K , the availability of accurate real-time S_f data in CCS opens the door to a commensurate improvement in K calculations. This also marks the beginning of a new age in predictable and

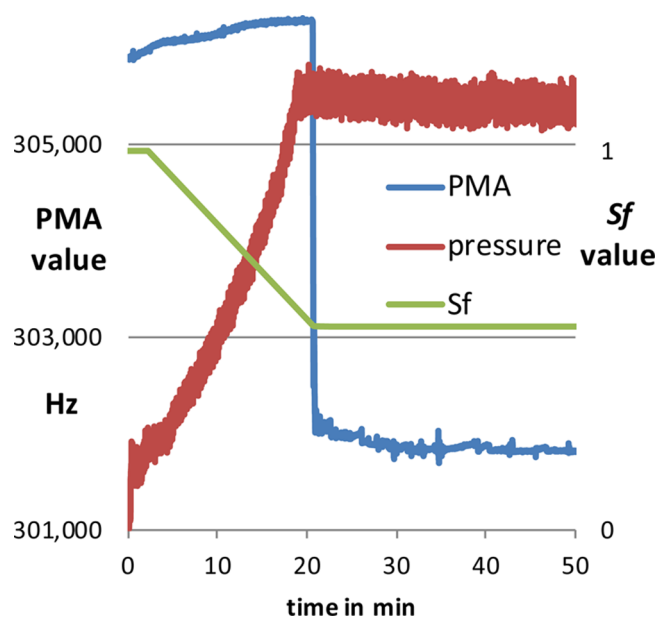


Figure 3. Signal changes during column equilibration. At time = 0, the lower (“mobile”) phase of a two-phase solvent system (HEMWat (4:6:5:5)) is introduced into a rotating column filled with the upper phase. A certain volume of upper (“stationary”) phase is displaced by the mobile phase until equilibration is attained. Blue = PMA value, red = pressure, and green = real-time stationary phase retention ratio (S_f).

reproducible CCS which adheres to straightforward equations that require readily accessible analyte parameters.

I3: Design of the CherryOne Instrument. Incorporating all of the information gathered during the development phase, together with the authors’ 40+ years of collective experience with existing CCS technology, a new CCS column control instrument was assembled (sections SI3 and SI8, Supporting Information). The main features of this instrument, called CherryOne, are (1) a redesigned chassis with smaller footprint, better accessibility, and solvent rack; (2) four pumps adapted with appropriate check valves for low-pressure use; (3) a fifth pump for effluent makeup solvent; (4) two motorized six-port valves; (5) in-line PMA with integrated temperature sensor; (6) UV detector with preparative flow cell; (7) pressure sensor; (8) makeup solvent pump; (9) a gas purge system; and (10) a fraction collector. All of the devices are controlled via *Corbel*, a custom-built, web-based data system that allows Internet/http-based remote instrument operation and enhances its automation capabilities: the operator can manipulate the instrument in real-time using a web browser, use any computer or mobile device, set up a run, and monitor its completion from any location. Within *Corbel*, the CherryOne read out can be selected and visualized graphically for spot-checking of the most important feedback parameters of an ongoing separation. A surveillance camera mounted near the solvent bottles allows visual monitoring of solvent levels. This control system may be interfaced with any available countercurrent separation instrument.

I4: Reproducibility and Validation of CCS via Temperature and Pressure/Viscosity Measurements. Many centrifugal CCS columns, including the one used in this project, provide temperature control mechanisms in order to remove the heat generated by the moving parts and stabilize the temperature. However, it cannot be assumed that the solvent flowing through the column is at the same temperature as the control

setting. Because the solvents are generally mixed and dispensed at room temperature, temperature differences inside of the column may affect both the two-phase equilibrium and the overall separation. By monitoring the effluent temperature, the CherryOne verifies that the cooling mechanism is working properly, detects a variety of temperature related issues early, and enhances reproducibility. As temperature also effects permittivity, these data can also be used to normalize the PMA signal when temperatures fluctuate between runs. Furthermore, the data system monitors, records, and displays the real-time pressure of the system. This allows detection of anomalies in the flow pattern that may indicate blockages or leaks. For protection, column-specific pressure limits may also be configured to stop the pumps in the case of overpressure. Figure SI12 of the Supporting Information shows that the pressure is directly proportional to the flow rate under column filling conditions. In addition, Figure 3 shows that an increase in the column pressure occurs during the column equilibration process. As the mobile phase exits the column ("break-through") to indicate that the equilibration is complete, the pressure levels off.

Practical Applications (A1–A3) of Automated CCS.

The following experiments carried out with the CherryOne demonstrate a few applications of automated CCS. Key aspects of the technology are addressed as follows: utility and data parameters of the PMA, which allows quantitative monitoring of the two phases, and enables real-time Sf calculation in CCS (A1); real-time determination of eluent *K* values (A2); and automation of the *K*-targeted fractionation of a complex natural product extract (A3).

A1: Real-Time Measurement of Sf. The PMA signals elicited by the upper and lower phases of a wide variety of solvent systems were evaluated and ultimately found to have an inverse relationship to the dielectric constants of the solvent components. Generally, solvent phases containing significant amounts of hexane and/or heptane tend to elicit more variable short-range (noisy) PMA signals than aqueous and/or alcoholic phases. The PMA values are stable and reproducible. The relative standard deviation of PMA values taken over a year's time for HEMWat 0 was $\ll 0.2\%$. This compares favorably ($>6\sigma$) with the average difference of PMA readings for the two individual phases. In addition, PMA values may provide a meaningful measure of solvent system overall polarity and/or quality.

The PMA works on the principle that there exists a significant difference in permittivity, and therefore signal values, between the two phases. Each time a new solvent system is run, the PMA values for the upper and lower phases are acquired. Once these two values are manually entered, the solvent phases are readily identified by the software. If the PMA value is between the two threshold values, the software records that a mixture of both upper phase and lower phase is leaving the column in a proportion to the distance between the two threshold values. Figure 4B shows that as the overall polarity of the solvent system increases (from heptane/MeOH to EtOAc/H₂O), the PMA values for both the upper and lower phase decrease. For other solvent systems studied, the PMA value differences between the two phases ranged from a high of 6,100 to a low of 2,500 PMA units.

The PMA values only need to be determined once per solvent system and are entered into the software method for the chromatographic run. Accordingly, an automated CCS run in EECCC mode is performed in three steps: (step 1) obtain

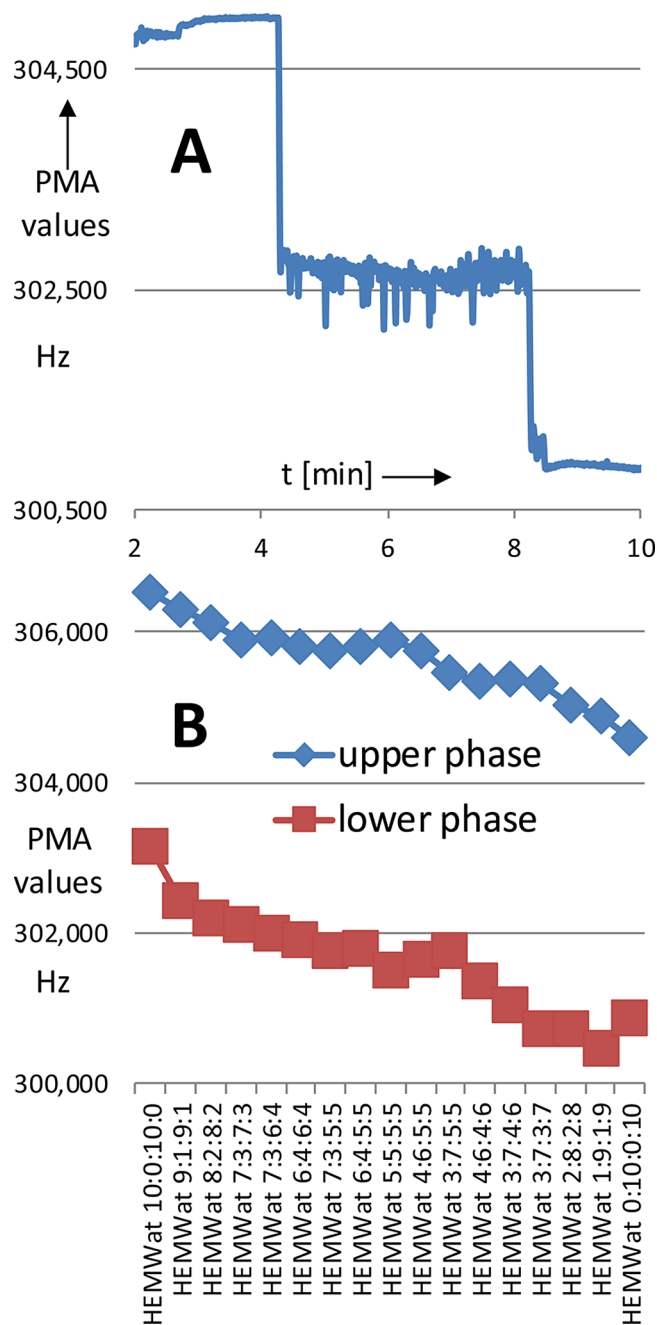


Figure 4. (A) PMA response for HEMWat 0 upper phase, followed by 1:1 mixture of upper and lower, followed by lower phase. (B) PMA values of upper and lower phases for the 17 solvent systems in the HEMWat family.

the PMA values for upper and lower phases; (step 2) fill the column with the stationary phase; (step 3) initiate the EECCC run with (a) simultaneous introduction of mobile phase and sample loop contents, (b) continuous elution with 1.0 column volume (V_C) of the mobile phase, and, finally, (c) completion of the run with $\sim 1.1V_C$ of the stationary phase (Figure 5). The last step, 3c, combines EECCC stages II + III, also known as sweep elution and extrusion, respectively.¹² It effectively extrudes the already-fractionated components in order and results in a system filled with pristine stationary phase, ready for another injection. The instrument totalizes eluted volumes of each solvent phase and calculates and graphs, in real time, the stationary phase ratio following eq 1.

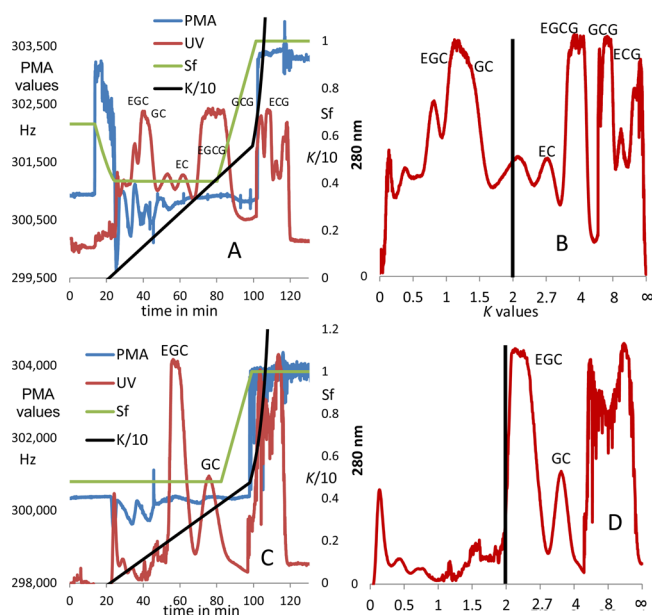


Figure 5. (A) Automated separation of 50 mg green tea catechins on a small-volume (~ 20 mL) hydrodynamic CCS instrument. Blue line = PMA values (y axis values on the left), red line = UV absorption at 280 nm, green line = Sf values (y axis values on the right), and black line = K values ($K/10$ y axis values on the right). CCS performed in a *ter*AcWat (5:5:10) solvent system with lower phase mobile: 0.5 mL/min flow rate; 2,000 rpm; 0.41 Sf minimum value; 20 °C. EGC = epigallocatechin, GC = galocatechin, EC = epicatechin, EGCG = epigallocatechin gallate, GCG = galocatechin gallate, and ECG = epicatechin gallate with corresponding K values of 1.1, 1.4, 2.7, 3.9, 5.6, and 7.8, respectively. (B) Reciprocal shifted symmetry K-plot of UV data in A. (C) Secondary fractionation of 41 mg green tea catechins. Blue line = PMA values (y axis values on the left), red line = UV absorption at 280 nm, green line = Sf values (y axis values on the right), and black line = K values ($K/10$ y axis values on the right). HEBuWat (1:4:5:10) solvent system with lower phase mobile: 0.5 mL/min flow rate; 2,000 rpm; 0.45 Sf minimum value; 20 °C. EGC = epigallocatechin and GC = galocatechin, with corresponding K values of 2.4 and 3.4, respectively. Recovery was 22 and 8 mg, respectively. (D) Reciprocal shifted symmetry K-plot of UV data in C, showing the typical linear increase in K until the EECCC midpoint at $K = 2$, and the nonlinear (reciprocal) increase of K values thereafter.

The proportionality of the PMA signals to the relative composition of the phases also opens the opportunity to use the PMA for the monitoring of eluents in gradient CCS. Whereas the nature of changing solvent composition in gradients inevitably forfeits the ability to calculate K values, the PMA has a distinctive utility as a generic phase detector and can potentially provide a new means of defining gradient conditions in CCS.

A2: K Plots. Real-time K values are calculated and graphed based on mobile and stationary phase volumes that are informed by the PMA. Partition coefficient values are calculated in real time using eqs 2 and 3 with corrections for extracolumn volumes,⁴ which tend to be insignificant on larger instruments.

The main advantage of employing the PMA is that the loss of stationary phase during equilibration and also during a separation run may be monitored and immediately incorporated into Sf and K calculations. Once the run has been completed, the raw data from each data stream may be recovered as a *.csv file and graphed in the appropriate software application. Each method is stored and may be rerun or copied

and modified for future runs. Taking into account the preceding considerations, K-plots are completely normalized and comparable between any instrument or experiment. In addition, K-plots can readily reveal differences in the resolving power of various CCS instruments by noting the relative peak width.

A3: Automated K-Targeted CCS Fractionation of Green Tea Catechins. The separation of catechins from green tea illustrates how real-time monitoring of PMA values, UV absorbance, Sf values, and K values work in tandem to create a rational process that may be easily monitored and verified by the operator. Figure 5A shows the fractionation of a 50 mg sample of polyphenol-enriched crude extract on a preequilibrated 17.9 mL CS column. The *ter*AcWat 5:5:10 solvent system was chosen for initial fractionation of the crude sample. The chromatograms in Figure 5 show the UV absorption and PMA signal traces in the form of raw data. The Sf and K data are calculated values based on input (high and low PMA cutoff values as well as initial Sf) and real-time PMA and pump data. Sf calculations are based on what phase is being pumped into the column and what phase, or mixture of the phases, that the PMA detects at the column outlet. The real-time K values are based on the Sf data and the EECCC stage (eqs 2 and 3). As is typical with crude extracts, in this separation, significant loss of stationary phase was observed prior to the elution of unretained analytes. The Sf was adjusted accordingly from its initial value of 0.65. The PMA response to polar analytes accompanied by a drop in PMA values was also observed from 25 to 45 min of this reversed-phase run. The Sf may be seen to level off at 0.41 as the analytes elute. At 80 min the mobile phase being pumped into the column is replaced by the initial stationary phase and the Sf begins to increase. This is the beginning of the EECCC stage II “sweep elution.” The eventual breakthrough of the stationary phase at 102 min was recorded by the PMA at the start of the extrusion stage. The K value calculations are then adjusted according to the stage III extrusion (eq 3) and begin to rise rapidly until they (theoretically) reach infinity at the end of the run. Figure 5B represents the reciprocal shifted symmetry K-plot with the midline at $K = 2$ for the UV data shown in Figure 5A.

Because the green tea catechins, EGC and GC, nearly coeluted in the *ter*AcWat solvent system, a secondary fractionation was carried out with HEBuWat 1:4:5:10 as an orthogonal solvent system,⁷ employing otherwise identical operating conditions as the primary fractionation (Figure 5C). In contrast to the previous separation, there was no detectable stationary phase loss after the equilibration of the column. This pattern is fairly common in CCS, where crude extracts tend to emulsify the biphasic solvent system and lead to stationary phase loss, while prefractionated samples tend to be more soluble and, thereby, impart minimal disruption to the biphasic solvent system. Similar to the previous separation, a noticeable but nondisruptive dip in the PMA values occurs between 20 and 40 min as the polar analytes elute. Figure 5D represents the reciprocal shifted symmetry K-plot with the midline at $K = 2$ for the UV data shown in Figure 5C. The recording of accurate K values ensures that these same analytes may be isolated from any source on any CCS instrument, with greater or lesser resolution, depending on the instrument.

CONCLUSIONS

This report describes the development and application of a CCS system featuring a new permittivity-based phase metering apparatus (PMA) that continuously totalizes the balance of the

column's stationary and mobile phases in real time. This permits instantaneous calculation of CCS's key experimental parameter, namely, Sf. The volumetric measures are subsequently incorporated into partition coefficient (K) calculations. For any solvent system, K values are intrinsic properties of analytes, and in CCS they empower facile, targeted purification. Moreover, proper K calculation fosters full normalization of the chromatographic x -axes in CCS.¹¹ In addition, utilization of modern CCS operation modes, such as EECCC, allow for the practical determination of K values for the complete range ($0 < K < \infty$) of analytes. The targeted purification of botanical reference materials such as the green tea catechins demonstrates the power of K -targeted preparative analysis. Finally, all sensing technology required to monitor key parameters is now available to enhance the reproducibility and validate CCS.

■ ASSOCIATED CONTENT

■ Supporting Information

Tables listing nomenclature and constitution of two-phase solvent systems, SIA sensor testing protocol, sensor evaluation results, operational parameter effects, summary of sample loadings and Sf measurements, and various parameters used; text describing manual determination of the stationary phase retention volume ratio and sample loading and stationary phase volume retention experiments, and figures showing a diagram of automated CCS; a photograph of the CherryOne instrument with integrated Corbel data system, optical characteristics of two-phase solvent systems; pressure sensor responses to five different solvent systems, effluent sensing capabilities, linear correlation of experimental PMA values; CCS system schematic diagram, screenshot of the real-time operation schematic of the CherryOne system, and comparison of PMA values and pressure in a column with increasing flow rate. The Supporting Information is available free of charge on the ACS Publications website at DOI: 10.1021/acs.analchem.5b01613.

■ AUTHOR INFORMATION

Corresponding Author

*Tel.: (312) 355-1949. E-mail: gfp@uic.edu.

Notes

The authors declare the following competing financial interest(s): S.M.P. is President of Cherry Instruments, a Division of Wrightwood Technologies Inc. S.M.P., L.R.C., T.B., L.P., W.F., N.N., and J.M. are shareholders and/or employees of Cherry Instruments. The other authors declare no conflict of interest.

■ ACKNOWLEDGMENTS

Support was received by grants R43AT004534 and R44AT004534 from NCCIH (formerly NCCAM) of the NIH. We are grateful to Dr. Martin Biendl and Mr. Harald Schwarz of Hopsteiner (New York, NY, USA, and Mainburg, Germany) and Dr. Kan He (formerly Naturex, South Hackensack, NJ, USA) for providing study materials and to Kalsec, Inc. (Kalamazoo, MI, USA) for providing CCS instruments for early development work.

■ DEDICATION

Dedicated to Dr. James B. McAlpine, a pioneer in the design and innovative use of countercurrent separation devices applied

to the discovery of new antibiotics, on the occasion of his 75th birthday.

■ REFERENCES

- (1) Pauli, G. F.; Pro, S. M.; Friesen, J. B. *J. Nat. Prod.* **2008**, *71*, 1489–1508.
- (2) Friesen, J. B.; McAlpine, J. B.; Chen, S.-N.; Pauli, G. F. *J. Nat. Prod.* **2015**, in press, DOI: 10.1021/np501065h.
- (3) Conway, W. D.; Petroski, R. J. *Modern Countercurrent Chromatography*; American Chemical Society: Washington, DC, USA, 1995.
- (4) Conway, W. D.; Chadwick, L. R.; Fong, H. H. S.; Farnsworth, N. R.; Pauli, G. F. *J. Liq. Chromatogr. Relat. Technol.* **2005**, *28*, 1799–1818.
- (5) Ito, Y.; Conway, W. D. *High-Speed Countercurrent Chromatography*; John Wiley & Sons: New York, 1996.
- (6) Chadwick, L. R.; Fong, H. H. S.; Farnsworth, N. R.; Pauli, G. F. *J. Liq. Chromatogr. Relat. Technol.* **2005**, *28*, 1959–1969.
- (7) Friesen, J. B.; Ahmed, S.; Pauli, G. F. *J. Chromatogr. A* **2015**, *1377*, 55–63.
- (8) Qiu, F.; Friesen, J. B.; McAlpine, J. B.; Pauli, G. F. *J. Chromatogr. A* **2012**, *1242*, 26–34.
- (9) Ramos Alvarenga, R. F.; Friesen, J. B.; Nikolic, D.; Simmler, C.; Napolitano, J. G.; van Breemen, R.; Lankin, D. C.; McAlpine, J. B.; Pauli, G. F.; Chen, S. N. *J. Nat. Prod.* **2014**, *77*, 2595–2604.
- (10) Liu, Y.; Chen, S. N.; McAlpine, J. B.; Klein, L. L.; Friesen, J. B.; Lankin, D. C.; Pauli, G. F. *J. Nat. Prod.* **2014**, *77*, 611–617.
- (11) Friesen, J. B.; Pauli, G. F. *Anal. Chem.* **2007**, *79*, 2320–2324.
- (12) Berthod, A.; Friesen, J. B.; Inui, T.; Pauli, G. F. *Anal. Chem.* **2007**, *79*, 3371–3382.
- (13) Ito, Y. *J. Chromatogr. A* **2013**, *1271*, 71–85.
- (14) Lu, Y. B.; Pan, Y. J.; Berthod, A. *J. Chromatogr. A* **2008**, *1189*, 10–18.
- (15) Trabelsi, N.; Oueslati, S.; Falleh, H.; Waffo-Teguo, P.; Papastamoulis, Y.; Merillon, J. M.; Abdelly, C.; Ksouri, R. *Food Chem.* **2012**, *135*, 1419–1424.
- (16) Shehzad, O.; Khan, S.; Ha, I. J.; Park, Y.; Kim, Y. S. *J. Sep. Sci.* **2012**, *35*, 1462–1469.
- (17) Peng, A. H.; Li, R.; Hua, J.; Chen, L. J.; Zhao, X.; Luo, H. D.; Ye, H. Y.; Yuan, Y.; Wei, Y. Q. *J. Chromatogr. A* **2008**, *1200*, 129–135.
- (18) Adelmann, S.; Schembecker, G. *J. Chromatogr. A* **2011**, *1218*, 5401–5413.
- (19) Subbaramaia, D. S. *Proc.-Indian Acad. Sci., Sect. A* **1934**, *1*, 355–362.
- (20) Wang, P. M.; Anderko, A. *Fluid Phase Equilib.* **2001**, *186*, 103–122.
- (21) Mohsen-Nia, M.; Amiri, H. *J. Chem. Thermodyn.* **2013**, *57*, 67–70.
- (22) Ma, L.; Nie, Z.; Huang, Y.; Yao, S. Z. *Sci. China: Chem.* **2010**, *53*, 1391–1397.
- (23) Chadwick, L. R.; Nikolic, D.; Burdette, J. E.; Overk, C. R.; Bolton, J. L.; van Breemen, R. B.; Fröhlich, R.; Fong, H. H. S.; Farnsworth, N. R.; Pauli, G. F. *J. Nat. Prod.* **2004**, *67*, 2024–2032.